POLISH MARITIME RESEARCH 3 (127) 2025 Vol. 32; pp. 66-78
10.2478/pomr-2025-0036

DESIGN OF A WAVE-SHAPED TOWING CABLE FOR STABLE, LOW-DRAG ACOUSTIC MONITORING IN WAVE GLIDER SYSTEMS

Yingyuan Tian [1, 2]
Yaxun Chen [2]
Yang Qi [1]
Yunfei Lv [2]
Weijia Li [1 *]
[1] School of Naval Architecture and Ocean Engineering, Huazhong University of Science and Technology, Wuhan, China
[2] College of Underwater Acoustic Engineering, Harbin Engineering University, Harbin , China

* Corresponding author: *liweijia@hust.edu.cn (Weijia Li)*

ABSTRACT

As wave-powered unmanned surface vehicles, wave gliders offer an effective platform for persistent marine acoustic monitoring. However, the deployment of deep-towed acoustic systems from these platforms is impeded by challenges such as hydrodynamic drag, motion instability, and flow-induced noise, particularly in elevated sea states. A novel acoustic towing system featuring a wave-shaped cable, with strategically distributed float-sinker pairs, is presented here. Its performance is optimised through parametric tuning of the wave number, wavelength, and amplitude to mitigate drag and suppress vortex-induced vibrations. To understand the complex dynamics of the system, a comprehensive hydrodynamic model combining Euler-Lagrange dynamics with computational fluid dynamics was developed. This integrated framework facilitated a systematic investigation of the critical cable parameters for effective drag reduction and suppression of vortex-induced vibrations. Simulations revealed that low-frequency disturbances induced larger attitude fluctuations in the towed body than their high-frequency counterparts. Furthermore, the vibration-damping effectiveness of the cable was found to increase with wave number, albeit at the cost of reduced towing speed. An analysis of the acceleration power spectral density revealed that a critical, speed-dependent trade-off among damping performance, system stability, and hydrodynamic drag governs the optimal float-sinker configuration. At low speeds (≤0.5 m/s), a configuration of 12–14 float-sinker pairs per wavelength yields superior overall performance. At higher speeds (≥1.0 m/s), a sparser configuration offers lower drag but risks resonant amplification, whereas a denser layout ensures stability at the expense of higher drag. This validation was substantiated by the alignment between the dominant response frequency of the towed body with wave excitation and the effective suppression of high-frequency vibrations. Collectively, these findings demonstrate that strategically configured towing cables can significantly enhance the operational performance of wave glider-based acoustic monitoring systems by improving hydrodynamic efficiency and mitigating flow-induced vibrations and their associated noise. The findings of this research provide a robust foundation for future studies of adaptive towing strategies and multi-body hydrodynamic interactions in marine environments.

Keywords: Wave glider; Acoustic towed array; Passive acoustic; Hydrodynamic; Wave-shaped cable; Vortex-induced vibration (VIV) suppression

INTRODUCTION

AMarine observation technologies are an essential aspect of ocean science and maritime operations. Of these technologies, wave gliders, also known as wave-powered unmanned surface vehicles (USVs), have emerged as a highly effective platform for persistent marine monitoring, as they offer exceptional endurance and broad spatial coverage in an economically viable manner. Their integration with underwater acoustic systems, in which sound propagation is leveraged for subsea information transmission, marks a significant advancement in oceanic exploration. The minimal self-noise generated by their mechanical propulsion makes wave gliders particularly suiTable for acoustically sensitive missions, such as the acquisition of data on ambient noise, biological vocalisations, and anthropophonic signatures to optimise sonar system performance.

However, the deployment of deep-towed acoustic systems from these low-power platforms gives rise to considerable hydrodynamic complexity. Although deep towing is necessary to mitigate surface wave-induced noise and thermocline effects, it inherently increases hydrodynamic drag and can induce motion instability in the towed body. These instabilities not only degrade the quality of sonar data by generating flow noise but also compromise the acoustic stealth and manoeuvrability of the vehicle [1]. Previous investigations have highlighted the efficacy of wave gliders for various acoustic applications, including passive and active monitoring [2], the provision of mobile gateways for underwater wireless sensor networks (UWSNs) [3], the mapping of soniferous fish soundscapes [4], the study of cetacean behaviour [5], and contributions to ecological and biodiversity monitoring [6]. Similar platforms such as the AutoNaut USV have been successfully used for marine mammal detection [7] and real-time passive acoustic beamforming [8]. Despite these advancements, however, the challenge of managing the hydrodynamic and vibrational consequences of deep towing persists.

To address this issue, researchers have developed sophisticated modelling techniques. Methodologies such as the Euler-Lagrange formalism [9, 10], nonlinear numerical models [11], the nodal position finite element method (NPFEM) [12], and coupled lumped mass-spring models (LMSM) with computational fluid dynamics (CFD) [13] have been employed to analyse cable configurations and dynamic responses. Concurrently, studies of system stability have used high-gain observers and singular perturbation methods to ensure robust control [14], while others have focused on simplifying the steady-state analysis [15]. A primary concern in these systems is vortex-induced vibration (VIV), a significant source of structural fatigue and flow-induced noise. Research into the mitigation of VIV has often focused on external add-ons, such as suppression sleeves that diminish response amplitudes [16–18] or the optimisation of buoyancy module configurations on risers [19]. However, these external solutions can introduce additional hydrodynamic complexity, increase the mass of the system, and pose operational challenges during deployment and recovery.

This highlights a critical research gap in respect to the lack of a holistic approach that integrates passive vibration damping directly into the cable's intrinsic architecture, thereby avoiding the drawbacks of external attachments. To address this gap, this study proposes and analyses an innovative wave-shaped towing cable, where strategically distributed float-sinker pairs form a geometry that functions as an inherent mechanical filter. The aim of this design is to achieve robust VIV suppression and motion stability while optimising hydrodynamic efficiency. This paper describes the comprehensive modelling of the integrated towed system, presents simulation outcomes under varying operational parameters, and provides validation through sea trials. The findings demonstrate that a strategically configured wave-shaped cable can significantly enhance the performance and reliability of wave glider-based acoustic monitoring systems, and can provide a robust foundation for next-generation, low-drag, and sTable underwater towing solutions.

The ensuing sections of this paper describe an investigation of a wave-shaped cable towing system. Section II introduces the system architecture and methodology, and furnishes an overview of an integrated acoustic towed system deployed from a wave glider. Section III gives an overview of multibody dynamical modelling and simulation, delineates the theoretical framework employed for analysis, and presents the simulation outcomes derived by systematically varying salient design parameters. Section IV describes the sea trials undertaken to corroborate the simulation outcomes and to evaluate the practical performance of the wave-shaped cable design. Section V presents a conclusion and future work, recapitulates the most salient findings, summarises the contributions of this research, and suggests prospective avenues for subsequent investigations aimed at further optimising the design and performance of wave glider-based acoustic towed systems.

SYSTEM DESIGN AND METHODOLOGY

SYSTEM OVERVIEW

The proposed integrated acoustic towing system consists of a towed body and a composite towing cable. The cable comprises a vertical segment that connects the wave glider to a submerged lead mass (the "lead fish"), and a horizontal segment, which is engineered to give a wave-shaped geometry through the strategic placement of buoyancy elements (floats) and ballast weights (Fig. 1). The cable is attached to the submerged glider below its centre of gravity via a watertight connector. The lengths of both cable segments can be configured to meet specific operational requirements.

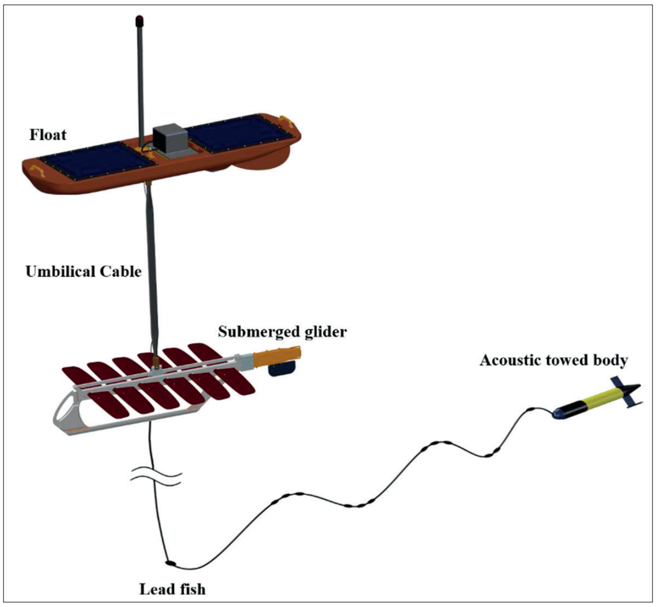

Fig. 1. Wave glider with acoustic towing system

A key innovation is the undulatory horizontal cable, which is formed by combining floats and weights to achieve near-neutral buoyancy. This design enhances the mechanical flexibility of the system, enabling it to dissipate vibrations induced by surface waves and ocean currents, which in turn minimises the motion perturbations transferred to the towed body, thereby providing a sTable platform for the acoustic payload. The lead fish provides the negative buoyancy necessary to maintain the system at its target operational depth. The undulatory geometry, defined by its wavelength and amplitude, can be optimised to tune the vibrational response of the system. To further mitigate hydrodynamic drag, the lead fish, floats, and ballast weights are all designed with streamlined profiles (Fig. 2).

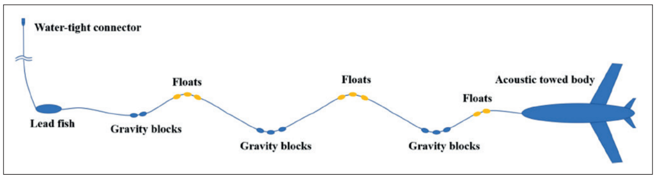

Fig. 2. Acoustic towing system

In contrast to rectilinear cables, a suboptimally configured undulatory cable can increase the system's overall drag, particularly under conditions of strong currents or high wave activity. A critical design objective is therefore to determine the optimal wave number, wavelength, and wave height to balance the competing demands of high stability and low drag for the wave-propelled USV. The baseline parameters of the system for the initial analysis are summarised in Table 1.

Tab. 1. Baseline parameters of the wave glider and acoustic towing system for initial analysis

Parameter	Value
Weight	100.0 kg
Float dimension	2.1 × 0.6 × 0.22 m
Submerged glider	2.0 × 1.1 × 0.4 m
Umbilical cable length	6.0 m
Diameter of towing cable	6.0 mm
Length of vertical section of towing cable	20–100 m
Length of horizontal section of towing cable	20 m
Length of towed body	966.0 mm
Maximum diameter of towed body	100.0 mm

Note: The parameters listed represent a typical baseline configuration. Specific parameters, such as the length of the horizontal section and the number of float-sinker pairs, were systematically varied in simulations to investigate their effects on the system dynamics, as detailed in Section III.

STABILITY OF THE TOWED BODY

The design of the towed body follows an iterative process that integrates performance specifications with CFD and stability validation, as outlined in Fig. 3. The process begins by defining the principal dimensions based on the sonar array requirements, which subsequently determine the minimum internal cavity diameter needed for the electronics. A preliminary design is then formulated.

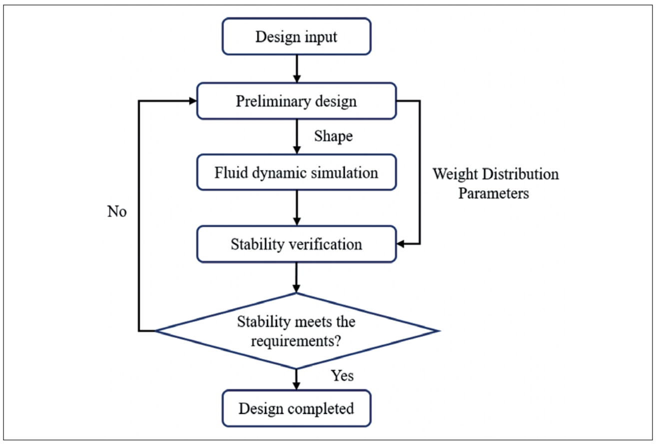

Fig. 3. Design process for the towed body

Using this preliminary model, CFD simulations (e.g. using Fluent) are performed to determine the body's hydrodynamic coefficients. These coefficients, along with the ballast mass parameters (mass, centre of mass, centre of buoyancy, etc.), are used to evaluate the static and dynamic stability of the body. The design-simulation-validation cycle is repeated until all performance and stability specifications are satisfied. The final design must not only meet stability criteria but also prioritise a compact, low-drag profile suiTable for towing by a power-constrained vehicle.

A stability analysis encompasses both static and dynamic criteria. Static stability requires a negative pitch moment coefficient $m_z^{\alpha} < 0$ to ensure that a restoring moment is generated when the body deviates from its equilibrium pitch angle. For a body in horizontal translation, the dynamic stability margin G_t must be positive, as defined by:

$$G_r = 1 - \frac{m_z^{\alpha}(\mu - C_y^{\overline{\omega}_z})}{C_y^{\alpha}(\mu \bar{x}_G - m_z^{\overline{\omega}_z})} > 0 \quad (1)$$

where $\mu = \frac{2m}{\rho SL}$ is a dimensionless mass coefficient, $C_y^{\overline{\omega}_z}$ is a non-dimensional factor of the lift angular velocity rotational derivative, C_y^{α} is the lift coefficient, $\bar{x}_G$ is the longitudinal position of the centre of gravity, and $m_z^{\overline{\omega}_z}$ is a non-dimensional pitching moment derivative.

From a structural perspective, the acoustic towed body is a streamlined body of revolution with distinct head, parallel mid-body, and tail sections. Stabilising fins with a specific airfoil are included at the rear of the body to serve as the mounting interface for the acoustic transducer array, as dictated by the acoustic array requirements. A preliminary design scheme for the towed body is depicted in Fig. 4.

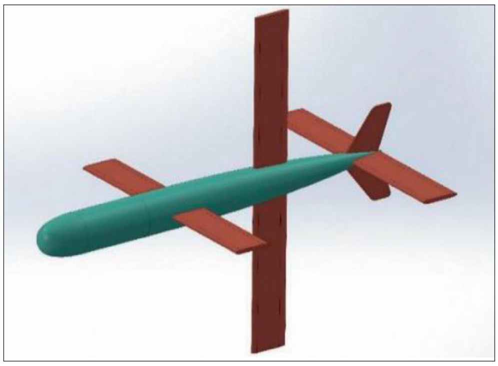

Fig. 4. 3D rendering of the shape of the acoustic towing body

The fluid dynamic parameters of the acoustic towed body were calculated using the commercial software platform Fluent. Typical pressure and velocity cloud maps for the towed body are shown in Figs. 5 and 6.

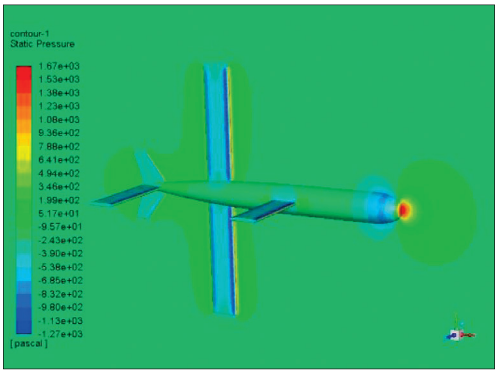

Fig. 5. Typical pressure cloud map for the acoustic towed body

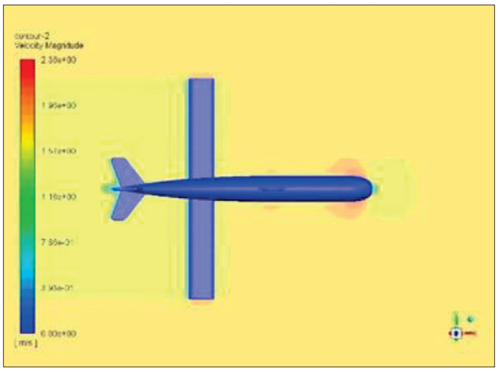

Fig. 6. Typical velocity cloud map for the acoustic towed body

The calculated results of the fluid dynamic parameters of the acoustic towed body are shown in Table 2.

Tab. 2. Fluid dynamic parameters for the acoustic towed body

Parameter	Value	Parameter	Value
C_y^{α}	0.35	$\bar{x}_G$	0.005
m_z^{α}	−0.028	C_y^{β}	−0.34
μ	0.022	m_y^{β}	−0.054
$C_y^{\bar{\omega}_z}$	−0.045	$C_y^{\bar{\omega}_y}$	−0.126
$m_z^{\bar{\omega}_z}$	−0.045	$m_y^{\bar{\omega}_y}$	−0.033

According to the criteria for the static stability and dynamic stability margins, $m_z^{\alpha} = -0.028 < 0$ and

$$G_q = 1 - \frac{m_z^{\beta}(\mu + C_z^{\bar{\omega}_y})}{C_z^{\beta}(m_y^{\bar{\omega}_y} - \mu \bar{x}_G)} = 1 - \frac{-0.054\times(0.022-0.0126)}{-0.34\times(-0.033-0.022\times0.005)} = 1.0449 > 0 \quad (2)$$

The simulation results demonstrate that the proposed acoustic towed body design exhibits excellent performance in terms of both static and dynamic stability within the longitudinal plane.

MULTIBODY DYNAMICAL MODELLING AND SIMULATION

MODELLING OF COMPLEX MULTIBODY DYNAMICS

A complex towing system can be discretised into multiple rigid-body elements interconnected via kinematic joints. This methodology uses well-established theories of multibody dynamics and numerical algorithms to handle the nonlinear phenomena and large deformation effects intrinsic to such systems. Each rigid-body element is associated with an independent local coordinate system in order to define its positional and orientational states in an unambiguous way. The kinematic constraints imposed by the joints allow these discrete elements to be integrated into a coherent dynamic system.

Based on the multi-body system modelling approach described above, the wavy cable is discretised into finite segments, which are then connected to form a multi-body system that is solved using multi-body dynamics methods. The towing cable is initially divided into a series of finite-length cable segments connected by nodes. The mass of the towing cable is concentrated at the centre of these cable segments, and the fluid resistance, additional mass, gravity, and buoyancy are also assumed to be concentrated at their centres. The nodes at both ends of each cable segment are connected to adjacent cable segments in a hinged manner, and stiffness and damping are added at the hinge to simulate the bending moment of the towing cable during bending. The wavy vibration-damping cable consists of three types of finite segments:

(1) Finite segment buoyancy block: The centre is located at the centre of the buoyancy block, and the two end nodes are located on circular cables on both sides of the buoyancy block;

(2) Gravity block finite segment: The centre is located at the centre of the weight block, and the two end nodes are located on circular cables on both sides of the weight block;

(3) Circular cable finite segment: The entire segment contains only circular cables, with the centre located at the centre of the finite segment.

The main process used to model the system is as follows.

The state vector of the connection point between any segment and hinge moving in space is defined as:

$$\boldsymbol{z} = [x, y, z, \phi, \theta, \psi, m_x, m_y, m_z, q_x, q_y, q_z, 1]^{\mathrm{T}} \quad (3)$$

where $[x, y, z]$ is the position vector of the connection point in the inertial frame; $[\phi, \theta, \psi]$ are the Euler angles representing its orientation (roll, pitch, yaw); $[m_x, m_y, m_z]$ are the internal moments exerted at the joint; and $[q_x, q_y, q_z]$ are the internal forces at the joint, all expressed in the inertial reference frame.

By deducing transfer equations and transfer matrices for typical elements and assembling these at the required locations, towed systems with various configurations can easily be modelled. The transfer matrices of elements can be developed directly from their dynamic equations using the linearisation methods mentioned in [20].

The transfer equation is expressed as:

$$z_{i+1} = U_i z_i \tag{4}$$

and the transfer matrix as:

$$U = \begin{bmatrix} I_3 & O_{3\times3} & O_{3\times3} & O_{3\times3} & O_{3\times1} \\ -U_{32}^{-1}U_{31} & O_{3\times3} & O_{3\times3} & -U_{32}^{-1}U_{34} & -U_{32}^{-1}U_{35} \\ O_{3\times3} & O_{3\times3} & O_{3\times3} & O_{3\times3} & O_{3\times1} \\ O_{3\times3} & O_{3\times3} & O_{3\times3} & I_3 & O_{3\times1} \\ O_{1\times3} & O_{1\times3} & O_{1\times3} & O_{1\times3} & 1 \end{bmatrix} \tag{5}$$

where I_k is the unit matrix, the subscript k denotes the order of the unit matrix, U_{31}, U_{32}, U_{34} and U_{35} are the sub-matrices of the transfer matrix of the outboard rigid body, and $O_{m\times n}$ is the state vector of the outboard end O of the rigid body.

The transfer vector can be obtained by Riccati transformation as:

$$z_i = S_i z_{n+1} + e_i \tag{6}$$

where S_i is the Riccati transfer matrix, and e_i is the Riccati transfer vector.

The recurrence relation is as follows:

$$\begin{cases} S_i = (U_{i,11} - U_{i,12} S_{i+1})^{-1} U_{i,12} \\ e_i = (U_{i,11} - U_{i,12} S_{i+1})^{-1} (e_{i+1} - U_{i,14}) \end{cases} \tag{7}$$

The present study focuses exclusively on the modelling and simulation of the motion responses of the towed system in the vertical plane, and environmental influences such as oceanic currents are explicitly excluded from consideration. This deliberate simplification isolates the fundamental hydrodynamic characteristics of the towed configuration, enabling a systematic analysis of its longitudinal dynamics through parametric investigation and numerical validation.

The entire towing damping cable consists of three types of finite segments connected in sequence to form a multi-body system. The buoyancy blocks and gravity blocks are clamped onto the towing cable using ellipsoidal half-blocks spaced at a specific distance. The finite segment model, which was developed based on the Modelica language [21], is depicted in Fig. 7.

The constant **Buoyancy** module applies the buoyancy of the finite segment to the centre of the finite segment through the **worldForce** module. The **Displacement force** module outputs the position force to the force module, via the input of the velocity feedback module **feedkVel**, and applies the position force to the centre of the finite segment. The **Damping force** module outputs the damping force to the **torque** module through the angular velocity feedback module **feedkAngu** as input, and applies the damping force to the centre of the finite segment.

The wave-shaped vibration damping cable is configured with a set of buoyancy blocks and gravity blocks (illustrated here with 16 buoyancy blocks and 16 gravity blocks as a representative example), which are strategically arranged along the towing cable, as illustrated in Fig. 8.

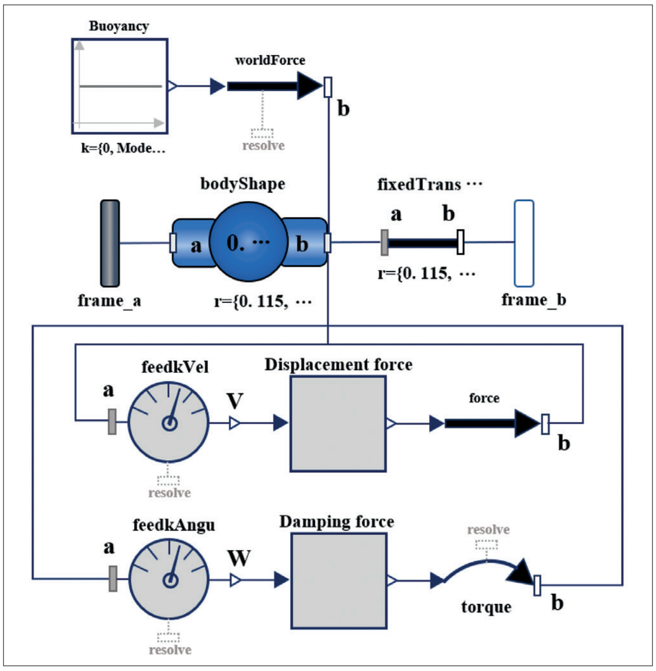

Fig. 7. Finite segment model of the wavy towing cable

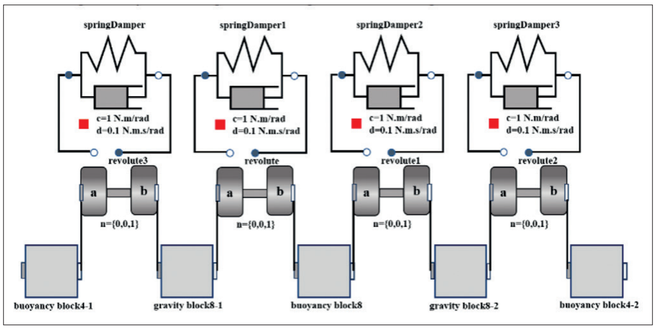

Fig. 8. Wave shaped damping cable model

springDamper is a spring damping module, whereas **revolute** is a hinge module, both of which are used to simulate hinge connections with stiffness and damping between two finite segments. **buoyancy block4-1** and **buoyancy block4-2** are both multi-stage cable models consisting of four floats and zeros between each pair of floats. **gravity block8-1** and **gravity block8-2** are multi-stage cable models consisting of ballast weights (with no elements) between each pair of ballast weights. **Buoyancy block8** is a multi-stage cable model consisting of eight floats (with no elements) between each pair of floats.

To illustrate the damping effect of the damping cable, we also established a model without damping, as shown in Fig. 9.

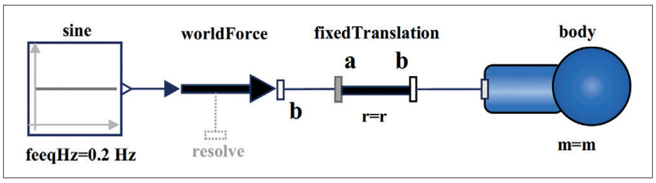

Fig. 9. Towing model without vibration damping

worldForce is the force application module that applies the drag force to the drag point. **fixedTranslation** is the structural dimension model that describes the displacement from the drag point to the floating center. **body** is the towing body model, and the connection interface is at the floating centre position. Finally, the drag damping effect is obtained through a joint simulation of the damping cable and the towing body.

A motion simulation model of a complex multi-body system comprising a wave glider and an acoustic towing system was developed using the Modelica language. The model was compiled and the simulation was implemented using the multidisciplinary simulation platform OpenModelica. Fig. 10 shows a diagram of the model.

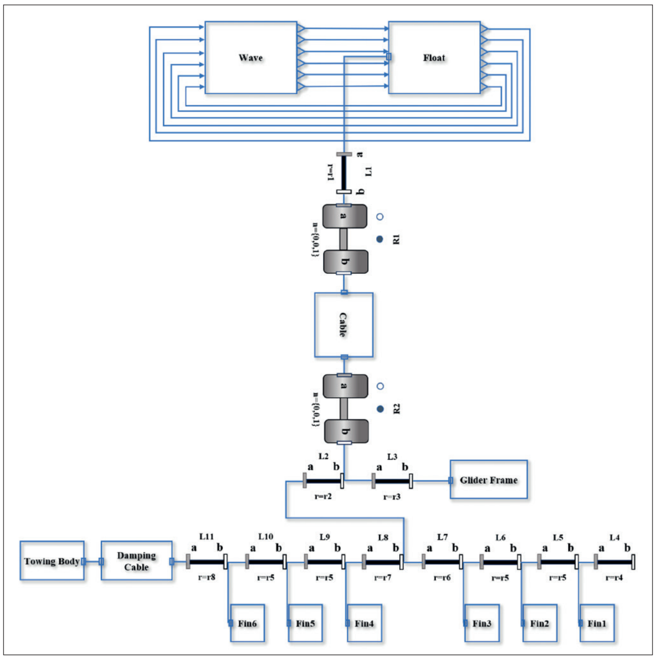

Fig. 10. Simulation model of the complex towing system between the wave glider and acoustic towing body

The complex towing system was constructed using the Modelica language and simulated using the multidisciplinary simulation platform OpenModelica 1.21.0 software, where:

- **Wave**: Wave force module
- **Float**: Six-degree-of-freedom motion module of the float
- **Cable**: Umbilical cable motion module
- **Glider frame**: Six-degree-of-freedom motion module of the submerged glider frame
- **Fin**: Six-degree-of-freedom motion module of a pair of flapping foils
- **Damping cable**: Wave-shaped damping cable model
- **Towing body**: Six-degree-of-freedom motion module for the towing body

The **Float** module outputs the displacement and attitude to the **Wave** module, which calculates the wave force on the platform based on the displacement and attitude of the platform near the water surface and outputs it to the **Float** module. The **Float** submodule and the **Umbilical Cable** submodule are connected by hinges, and the umbilical cable submodule is also connected to the submerged glider frame submodule via a hinge. The **Glider Frame** submodule representing the submerged glider is connected to six pairs of Fin1-6 submodules through hinges. At the same time, the **Glider Frame** submodule of the submerged glider frame is connected to the **Damping Cable** submodule of the damping cable via a hinge. Finally, the **Damping Cable** submodule is connected to the **Towing Body** submodule via a hinge, forming a complete complex multi-body system simulation model. L1 to L11 denote the structural dimensions of the respective cable segments, and r1 and r2 are hinge models.

This modular approach enables the individual components of the complex towing system to be modelled and simulated independently, which facilitates the development and optimisation of the overall system.

Analysis of vibration transmission and attenuation based on acceleration PSD

To quantify the efficacy of the wave-shaped cable in terms of suppressing vibration energy, the frequency-domain response of the towed system is investigated using power spectral density (PSD) analysis. The PSD S_{aa}(f) is computed using Welch's method from the vertical acceleration time series [22]. The vibration transmissibility between the towed body and the wave glider is then defined as:

$$S(f) = \frac{A_{out} - (f)}{A_{in} - (f)} \tag{8}$$

Energy attenuation at a specific frequency is determined by the following equation:

$$\text{Attenuation}(f) = 10log_{10}\left(\frac{A_{in} - (f)}{A_{out} - (f)}\right) \tag{9}$$

This metric provides an intuitive reflection of the vibration reduction effect at critical frequencies, facilitating straightforward cross-comparisons.

Simulation conditions and results

(1) Simulation conditions

Simulation conditions were configured to represent three distinct sea states: a calm sea (Case 1) and a moderate sea (Cases 2 and 3). The wave parameters for each simulation condition are summarised in Table 3.

Tab. 3. Wave parameters for various simulation conditions

Simulation case	Wave amplitude	Waveperiod
1	0.5 m	3 s
2	1.0 m	4 s
3	2.0 m	8 s

The configuration of the towing cable is summarised in Table 4.

Tab. 4. Configuration of the towing cable

Parameter	Value
Vertical section length of towing cable	40 m
Horizontal section length of towing cable	20 m
Wave Number of towing cable	2
Configuration of single wave	8 floats and 8 sinkers per wave

(2) Effect of towing speed

The towed cable system was configured with an initial depth of 40 m, and included a 20 m horizontal damping segment in the towing direction. The system design employed two complete wavelengths, with each wavelength containing periodic arrangements of eight floats and eight sinkers. Numerical simulations were conducted at four towing velocities: 0.3, 0.5, 1.0, and 1.5 m/s. The wave environment was characterised by regular waves with amplitude 1.0 m and period 4 s. The steady-state configurations of the towed cable under different towing speeds, as obtained from the simulations, are presented in Fig. 11.

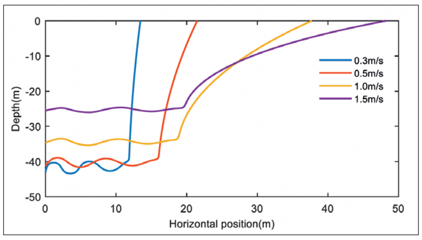

Fig. 11 Steady-state configurations of the towed cable system at varying towing speeds

The steady-state configuration of the towed cable system strongly depends on the towing velocity. Numerical simulations reveal that within the low-speed regime (0.3–0.5 m/s), the terminal depth of the cable remains sTable at approximately 40 m, corresponding to the initial preset depth. However, as the towing velocity increases to 1.0 m/s, the terminal depth decreases to 34 m, and a further rise in velocity to 1.5 m/s results in a pronounced reduction to 25 m. This phenomenon occurs due to hydrodynamic effects: increasing the towing velocity in a nonlinear manner augments the hydrodynamic lift forces, which in turn causes the terminal depth to decrease monotonically as the velocity increases.

(3) Effects of wavenumber configuration variations

Three distinct cable deployment strategies were systematically developed for vibration mitigation, which can be categorised based on the wavelength configuration as tri-wavelength (λ=3), bi-wavelength (λ=2), and mono-wavelength (λ=1) arrangements, as detailed in Fig. 12. The geometric parameters were specifically defined as follows:

Tri-wavelength configuration: This featured a horizontal drag segment of 30 m, which was optimised for distributed load dissipation.

Bi-wavelength system: This spanned 25 m, and balanced structural integrity with hydrodynamic efficiency.

Mono-wavelength design: This was constrained to 13 m for a concentrated stress distribution.

Notably, all configurations maintained a uniform wave amplitude of 1 m through the use of precisely calibrated float-sinker pairs, thus ensuring consistent dynamic baseline conditions for the experimental groups. This parametric differentiation enabled a systematic evaluation of the wavelength-dependent vibration attenuation mechanisms in the marine towing system.

Numerical simulation results demonstrating the effects of discrete wavenumber configurations on the pitch angle and horizontal velocity of the acoustic towed body under varying operational conditions are presented below.

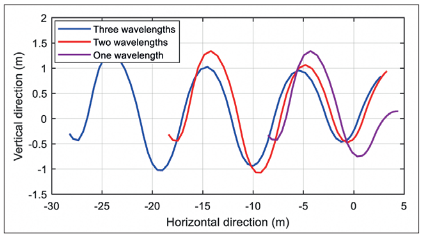

Fig. 12. Different wave number configurations at the same instant

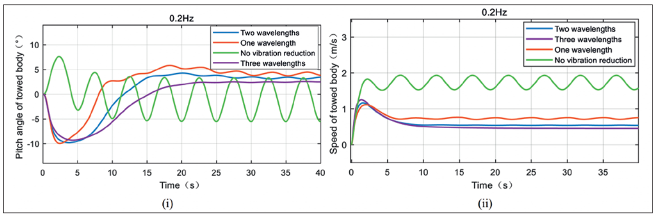

Fig. 13. (i) Pitch angle and (ii) speed of the towed body with different damping configurations at 0.2 Hz

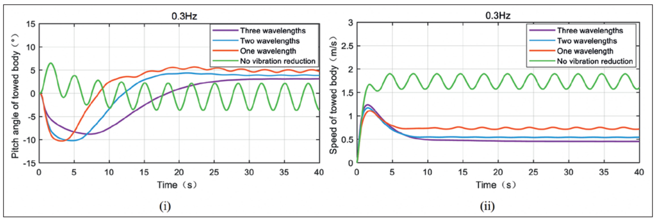

Fig. 14. (i) Pitch angle and (ii) speed of the towed body with different damping configurations at 0.3 Hz

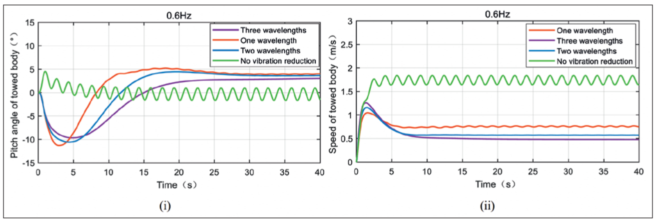

Fig. 15. (i) Pitch angle and (ii) speed of the towed body with different damping configurations at 0.6 Hz

The simulation results indicate that low-frequency interference forces induce larger attitude fluctuations in the towed body compared to high-frequency interference forces. However, the influence of the interference frequency on the average towing speed is relatively minor. Furthermore, the damping effect increases with the number of waves in the damping cable, but this increase is accompanied by a reduction in the average towing speed. Hence, an optimal balance between the damping performance and its impact on towing speed must be achieved. The selection of the wave number for the damping cable should be predicated on the towing capacity of the wave glider. In this study, a vibration damping cable configuration with two wavelengths was chosen to address this trade-off.

(4) Impact of waveform characteristics

Based on the method of PSD analysis, a systematic analysis of the wave-induced vibration damping effect under different float/sinker configurations was conducted. The dynamic response of the end of the towed cable was investigated at four towing speeds: 0.3, 0.5, 1.0, and 1.5 m/s. A two-wavelength configuration was employed for the vibration damping cable, and six different float/sinker configurations were designed as described in Table 5.

Tab. 5. Configurations of the damping cable

Case	Configuration details
Case A	16 floats and 16 sinkers per wavelength
Case B	14 floats and 14 sinkers per wavelength
Case C	12 floats and 12 sinkers per wavelength
Case D	10 floats and 10 sinkers per wavelength
Case E	8 floats and 8 sinkers per wavelength
Case F	6 floats and 6 sinkers per wavelength

The results indicate that at all speeds (0.3, 0.5, 1.0, and 1.5 m/s), all configurations yield excellent isolation performance at the primary excitation frequency of the tug (0.25 Hz). The values of S(f) are significantly less than one, with attenuation values typically ranging between 20 and 40 dB. This demonstrates that the wave-shaped cable system effectively isolates direct low-frequency disturbances from the tug, thereby providing a sTable operational environment for the towed body.

A critical finding is that when the number of float/sinker pairs in a single-wave configuration is less than 14, the system exhibits significant resonant peaks near the harmonics of the excitation frequency (e.g. 0.5, 0.75, 1.0 Hz), where the transmissibility exceeds one. This means that at these specific frequencies, vibration is not suppressed but is instead considerably amplified, which could lead to damage to the towed body or its internal equipment. This phenomenon suggests the risk of coupling between the cable's natural frequencies and the excitation harmonics, particularly as the number of floats/sinkers decreases, meaning that these resonant bands must be closely monitored.

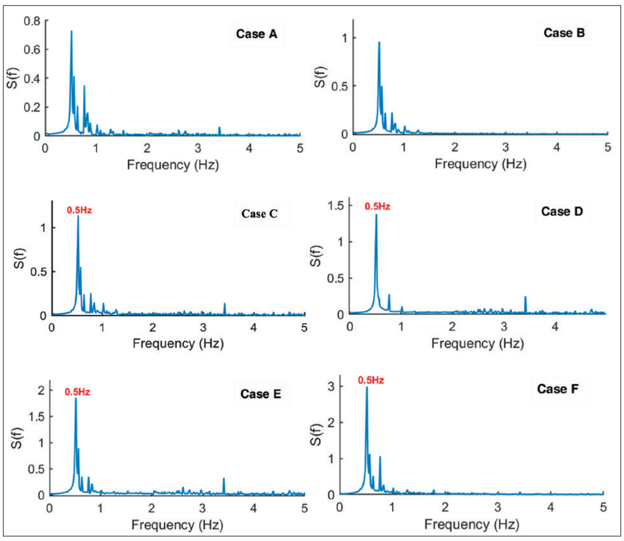

Fig. 16. Frequency-transfer curves for different configurations (0.3 m/s)

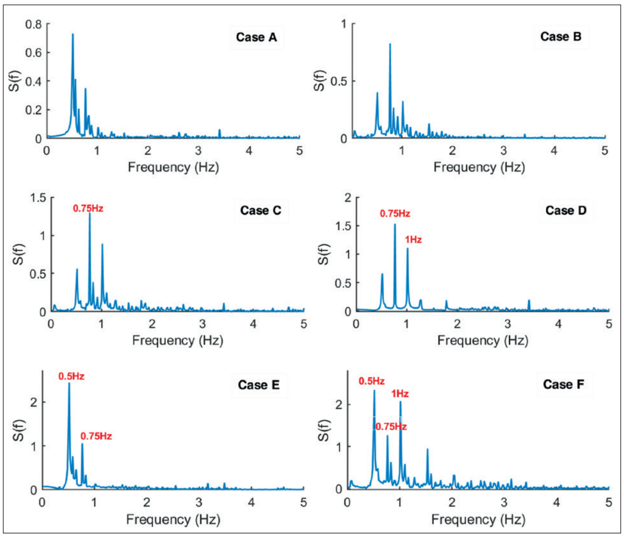

Fig. 17. Frequency-transfer curves for different configurations (0.5 m/s)

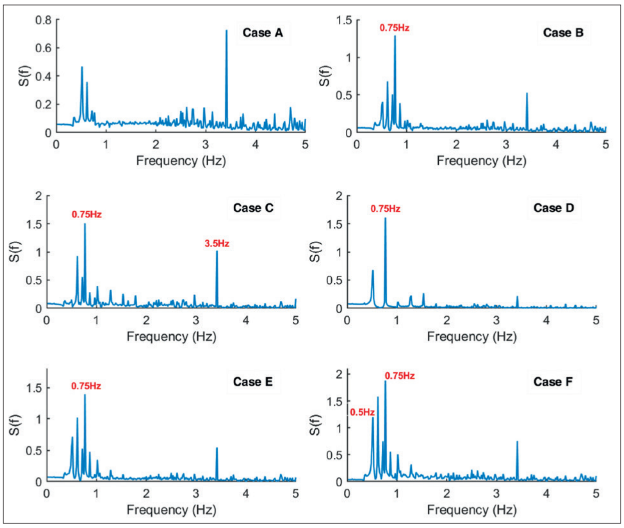

Fig. 18. Frequency-transfer curves for different configurations (1.0 m/s)

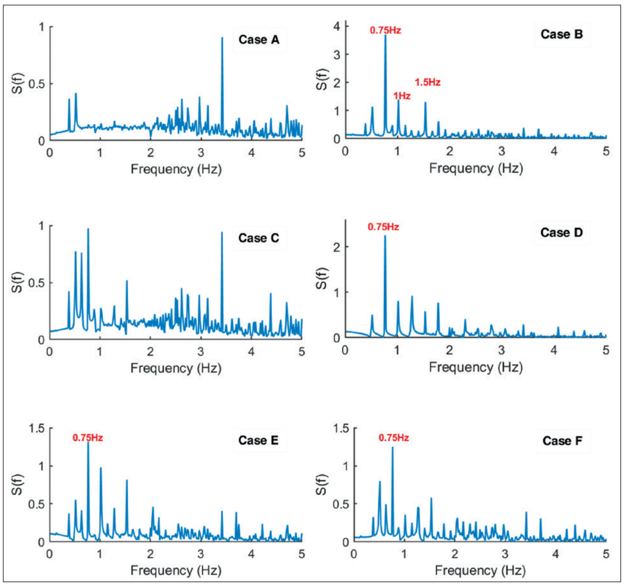

Fig. 19. Frequency-transfer curves for different configurations (1.5 m/s)

Tab. 6. Vibration damping effect for different configurations

Case	Frequency (Hz)	Attenuation (0.3 m/s)	Attenuation (0.5 m/s)	Attenuation (1.0 m/s)	Attenuation (1.5 m/s)
A	0.25	33.60	33.60	25.15	22.30
B	0.25	33.71	40.44	24.55	17.96
C	0.25	32.19	36.70	23.47	20.95
D	0.25	30.12	33.91	22.79	19.99
E	0.25	27.52	27.10	23.54	21.31
F	0.25	26.47	28.55	28.54	23.79

An analysis of the vibration transmissibility and attenuation indicates a critical, speed-dependent trade-off governing the optimal float-sinker configuration, which must balance the vibration damping performance, system stability, and hydrodynamic drag.

Under low-speed (≤0.5 m/s) conditions, a dense arrangement of 12–14 float-sinker pairs per wavelength delivers the most robust performance, offering effective vibration suppression with only a marginal and accepTable increase in drag. At higher speeds, a clear dichotomy emerges based on mission priorities.

For low-drag operations: A sparse configuration of six pairs is optimal, as this gives the lowest hydrodynamic drag and the most effective damping at the primary frequency. However, this configuration is susceptible to resonant amplification at harmonic frequencies. This vulnerability is attributed to its lower inherent structural damping and natural frequencies that are prone to coupling with flow-induced harmonic excitations, a risk amplified by potential VIV at higher velocities.

For maximum stability: To eliminate the risk of resonance entirely, a denser configuration (e.g., Case A) is required. This ensures stability across all conditions but at the cost of significantly higher drag.

Ultimately, these results confirm that no single configuration is universally optimal. The design choice involves a mission-specific optimisation in which these competing factors are strategically balanced against the anticipated operational profile to achieve the desired reduction in towed body motion.

(5) Simulation results for the complex towing system

Simulations of the motion of the complex towed system under various sea states were conducted to evaluate the key parameters, including pitch angle and horizontal velocity, for the system's primary components: the buoy, submerged glider, and the towed body. The simulation results are shown below.

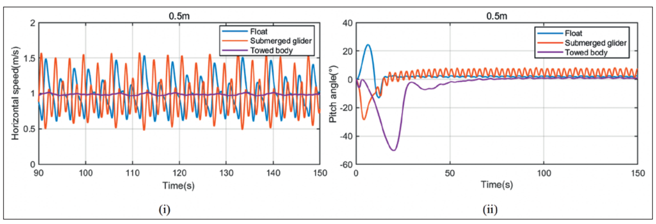

Fig. 20. (i) Horizontal speed and (ii) pitch angle for the complex towing system at 0.5 m wave amplitude

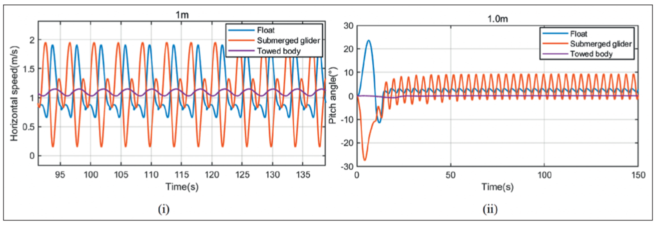

Fig. 21. (i) Horizontal speed and (ii) pitch angle for the complex towing system at 1.5 m wave amplitude

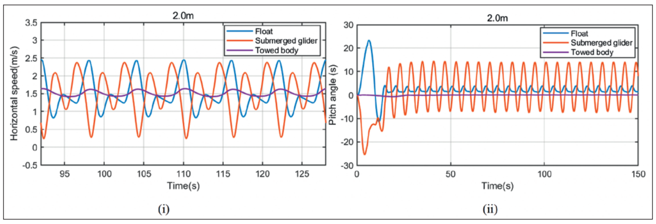

Fig. 22. (i) Horizontal speed and (ii) pitch angle for the complex towing system at 2.0 m wave amplitude

To minimise transient effects and ensure accurate statistical representation, a sTable period from 100 s to 140 s was extracted from the simulation data. Statistical results for the velocity and pitch attitude under various sea conditions are summarised in Table 7.

Tab. 7. Statistical results for velocity and pitch angle under various sea conditions

Wave amplitude (m)		Mean speed (m/s)	Speed ATR (m/s)	Mean pitch angle (°)	Pitch a ngle ATR (°)
0.5	F	0.9980	0.2216	1.8650	1.4690
	S	0.9789	0.3444	4.9373	2.8515
	T	0.9860	0.0143	0.8358	0.3079
1.0	F	1.1177	0.7960	2.3878	0.7804
	S	1.0549	0.5862	4.2156	5.1932
	T	1.0916	0.0563	0.0119	0.0148
2.0	F	1.5165	0.9217	2.1240	1.8312
	S	1.4628	0.7801	3.8374	10.1960
	T	1.5051	0.1214	0.0126	0.0320

In Table 7, the notations F, S, and T represent the float, submerged glider, and towed body, respectively. To quantify the magnitude of the fluctuations, the average true range (ATR) is used. Under relatively quiescent sea states, the velocity induced by the complex towing system interacting with the wave dynamics has a positive correlation with wave amplitude. The mean velocities of each component remain largely consistent. However, the amplitude of velocity fluctuation for the towed body (T) is demonstrably lower than for both the float (F) and the submerged glider (S). This observation suggests a more sTable velocity profile for the towed body, indicative of reduced sensitivity to wave-induced perturbations.

SEA TRIALS

The prototype of the wave glider and acoustic towing system is shown in Fig. 23.

Fig. 23. Prototype of the wave glider and acoustic towing system

The experimental site is illustrated in Fig. 24. The experiment spanned a duration of more than 72 hours, during which time the sea state remained relatively calm, with an average wave heights ranging from 0.7 to 1.3 m and an average wave period of 7–8 s. The mean wind speed was 7.6 knots. Ocean current velocities ranged from 0.1 to 0.7 knots, with periodic variations in the flow direction.

Fig. 24. Area used for the sea trials

Three sTable time segments were selected from the experimental data to generate time-domain and frequency-domain representations of the pitch and roll angles for the acoustic towed body. A time-domain analysis revealed a mean pitch angle of 2.1° and a mean roll angle of 0.71°. The limited variation in these attitude angles indicates that the towed body maintained a relatively sTable orientation under the prevailing sea conditions. A frequency-domain analysis showed a dominant frequency of 0.12 Hz for the pitch angle, a value that is closely aligned with the wave frequency of 0.125 Hz observed during the sea trial. This agreement validates the experimental results, and suggests that the attitude fluctuations for the acoustic towed body are primarily driven by wave excitation. Furthermore, the frequency-domain plots exhibited a paucity of harmonic components, with energy concentrated in the low-frequency range, indicating that the vibration-damping cable effectively suppressed high-frequency vibrations, thereby reducing attitude variations in the towed body and enhancing the overall system stability. The pitch and roll angles and their frequency-domain characteristics for the towed body in the different operational phases are shown in Figs. 25 to 30.

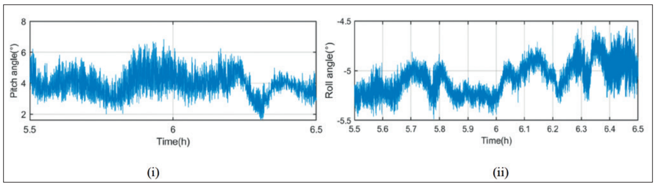

Fig. 25. Time-history curves for the (i) pitch angle and (ii) roll angle for the towed body (Time Segment I)

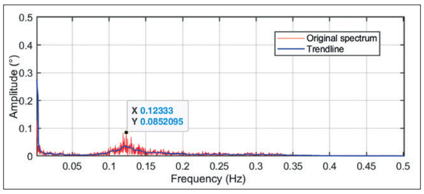

Fig. 26. Spectral characteristics of the pitch angle (Time Segment I)

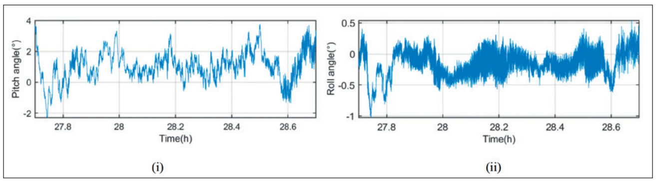

Fig. 27. Time-history curves for the (i) pitch angle and (ii) roll angle for the towed body (Time Segment II)

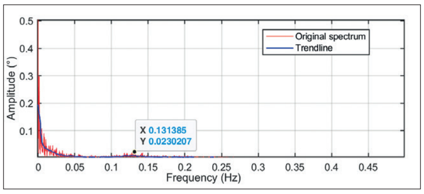

Fig. 28. Spectral characteristics of the pitch angle (Time Segment II)

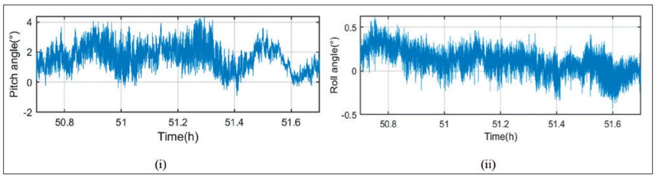

Fig. 29. Time-history curves for the (i) pitch angle and (ii) roll angle for the towed body (Time Segment III)

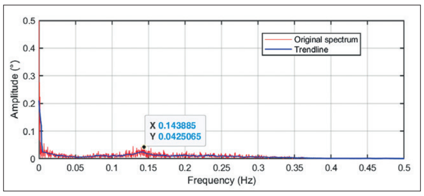

Fig. 30. Spectral characteristics of the pitch angle (Time Segment III)

The statistical results for the characteristic frequency, mean, and variance are shown in Table 8.

Tab. 8. Characteristic frequencies, means, and variances of pitch and roll angles for different time segments

Time segment (h)	Characteristic frequency (Hz)	Mean pitch angle (°)	Variance in pitch angle (°)	Variance in roll angle (°)
Segment I	0.123	3.8	0.687	0.027
Segment II	0.131	1.9	0.651	0.012
Segment III	0.144	0.688	0.801	0.02

A statistical analysis revealed a positive correlation between the mean pitch angle of the towed body and the wave height. Furthermore, the variance in the roll angle was significantly lower than for the pitch angle, indicating that the dynamic behaviour of the towed body is dominated by pitch motion. This observation is consistent with the typical motion characteristics of slender underwater towed bodies. A comparison of the characteristic frequencies across the three time segments revealed close agreement with the wave frequencies observed during the sea trial, confirming that the attitude variations of the towed body are primarily influenced by wave excitation. In addition, the frequency-domain plots exhibited a limited number of harmonic components, with energy concentrated in the low-frequency range; this suggests that the vibration-damping cable effectively suppressed high-frequency vibrations, thereby reducing the amplitude of the attitude variations for the towed body and consequently enhancing the overall system stability.

To validate the reliability of the simulation methodology, a comparative analysis was conducted between the simulation results and the sea trial experimental data, focusing primarily on the pitch angle, fluctuation amplitude, frequency characteristics, and vibration damping performance of the towed body. Reasonable agreement between the simulation and experimental values was confirmed through this analysis: for instance, during certain time segments, the pitch angle of the towed body remained below 1°. Furthermore, both the simulation and experimental results indicated that the dominant frequency of the end displacement response of the towed body coincided with the wave excitation frequency, providing preliminary validation of the accuracy of the simulation model. Further analysis of the simulation results indicated that optimising the configuration of the float/sinker system could effectively reduce the displacement response at the end of the towed body. The experimental results also confirmed that the vibration-damping cable effectively suppressed high-frequency vibrations, thereby reducing the amplitude of the towed body's attitude variations. When taken together, these findings show that the simulation model exhibited consistency with the experimental results in terms of the trend of the vibration damping performance, further validating the simulation model's effectiveness. This suggests that the simulation methodology is capable of predicting the dynamic behaviour of underwater towed systems with reasonable accuracy.

CONCLUSION AND FUTURE WORK

CONCLUSION

This study has successfully addressed the critical challenges of hydrodynamic drag, motion instability, and flow-induced vibration associated with deep-towed acoustic systems deployed from wave gliders. A novel passive towing system was introduced and validated, which incorporated a wave-shaped cable with strategically distributed float-sinker pairs. The primary contributions and key findings of this research can be summarised as follows:

1. An inherently damped cable architecture and a coupled modelling framework: A wave-shaped cable configuration was proposed as an effective passive mechanical filter to isolate the towed body from wave-induced disturbances. A comprehensive, integrated modelling framework was established in which CFD was used for component-level hydrodynamic characterisation and Euler-Lagrange-based multibody dynamics for system-level simulation. This framework was shown to be a robust tool for analysing the complex, coupled dynamics of the entire system.
2. Quantitative identification of a speed-dependent performance trade-off: A critical, speed-dependent trade-off among vibration damping, system stability, and hydrodynamic drag was quantitatively established. More specifically, an analysis of the vibration transmissibility and attenuation based on the acceleration PSD for the dual-wave configuration revealed that the optimal float and sinker arrangement was determined by a critical, speed-dependent trade-off between vibration damping, system stability, and hydrodynamic drag. At low speeds ($\leq$0.5 m/s), a dense configuration of 12–14 float-sinker pairs per wavelength provided overall performance, achieving excellent vibration attenuation of over 36.7 dB at the primary excitation frequency (0.25 Hz) while effectively mitigating the risk of harmonic resonance. Under high-speed conditions ($\geq$1.0 m/s), the design choice involved a critical trade-off: if low drag is the priority, a sparse configuration with six float-sinker pairs is preferable, with which the primary frequency attenuation can still reach approximately 28.5 dB but the risk of resonant amplification at harmonic frequencies must be accepted. Conversely, if system stability is the primary objective, a denser configuration is required to eliminate the risk of resonance, at the cost of sacrificing some low-drag performance. This finding provides clear, data-driven design guidelines for configuration of the system based on operational speed.
3. Comprehensive sea-trial validation of system performance: Extensive sea trials validated the practical feasibility and performance of the proposed system. The experimental data confirmed that the system maintained a highly sTable attitude for the towed body, even under in dynamic sea conditions. The filtering effect of the wave-shaped cable is exceptionally significant: both simulation and sea trial results indicate that compared to the surface float, the motion stability of the towed body is vastly improved. For instance, under simulated sea conditions with a 2.0 m wave amplitude, the attitude fluctuation (ATR) of the towed body was reduced by over 98% compared to the surface float, and its velocity fluctuation was reduced by approximately 87% (calculated from the data in Table 7), which powerfully demonstrates the effectiveness of our design.

In conclusion, this research has shown that a strategically configured wave-shaped towing cable can significantly enhance the performance and reliability of a wave glider-based acoustic monitoring system. The methodology and findings presented here provide a solid theoretical and practical foundation for designing next-generation, low-drag, and stable underwater towing systems.

LIMITATIONS AND FUTURE WORK

Although this work makes significant contributions to this field, certain limitations are acknowledged that suggest promising avenues for future research.

1. Although the dynamic model is comprehensive, it is primarily focused on the longitudinal (in-plane) motion of the system under regular wave conditions, which simplifies the complexities of real-world, three-dimensional sea states.
2. An analysis identified a risk of resonance at harmonic frequencies, but a dedicated modal analysis was not performed to precisely characterise the system's natural frequencies and mode shapes.
3. The configuration of the float-sinker pairs was determined through a parametric study rather than with a formal, multi-objective optimisation algorithm, which might yield further performance improvements.
4. The sea trials were conducted in relatively calm sea states (wave heights 0.7–1.3 m). While these trials were crucial for validating the fidelity of the simulation model and the system's fundamental stability under operational conditions, further experimental validation in more elevated sea states will be necessary to comprehensively assess the system's performance limits and its effectiveness in mitigating disturbances under the full range of intended operational scenarios.

FUTURE WORK

Based on the findings presented here, the following research directions are proposed:

1. Development of a six-degree-of-freedom spatial dynamic model: Future work should focus on developing a comprehensive six-degree-of-freedom model to investigate the system's spatial manoeuvrability, including its turning characteristics and spiral stability. This advanced model should incorporate irregular wave spectra and three-dimensional ocean currents to more accurately predict system behaviour in realistic operational scenarios.
2. System resonance characterisation and VIV coupling analysis: A dedicated investigation into the structural dynamics of the system is warranted. This could involve numerical techniques, such as the finite element method for modal analysis, or experimental modal analysis. The goals would be to precisely map the system's natural frequencies and to understand the risks of coupling between these frequencies, VIV phenomena, and dominant wave energy bands.
3. Adaptive configuration and multi-objective optimisation: To transcend the limitations of static configurations, future research could explore adaptive towing systems in which the parameters (e.g. cable shape or damping) are capable of being altered in real time. Furthermore, multi-objective optimisation algorithms (e.g. genetic algorithms) could be employed to explore the vast design space in a systematic way, to identify globally optimal configurations in which drag, stability, and damping performance are balanced across a wide range of sea states and towing speeds.

REFERENCES

1. Liu W et al. The flow-induced structural vibration noise suppression mechanism of a wing–plate model by the junction suction and trailing edge blowing. J. Sound Vib. 2024, Vol. 578, p. 118340. https://doi.org/10.1016/j.jsv.2024.118340

2. Bingham B et al. Passive and active acoustics using an autonomous wave glider. J. Field Robot. 2012, Vol. 29, pp. 911-923. https://doi.org/10.1002/rob.21424

3. Fedorova TA, Ryzhov VA, Semenov NN et al. Optimization of an underwater wireless sensor network architecture with wave glider as a mobile gateway. J. Mar. Sci. Appl. 2022, Vol. 21, pp. 179-196. https://doi.org/10.1007/s11804-022-00268-9

4. Luczkovich JJ, Sprague MW. Soundscape maps of soniferous fishes observed from a mobile glider. Front. Mar. Sci. 2022, Vol. 9, p. 779540. https://doi.org/10.3389/fmars.2022.779540

5. Bittencourt L et al. Map cetacean sounds using a passive acoustic monitoring system towed by an autonomous wave glider in the Southwestern Atlantic Ocean. Deep Sea Res., Part I, Oceanogr. Res. Pap. 2018, Vol. 142, pp. 58-68. https://doi.org/10.1016/j.dsr.2018.10.006

6. Ross SRPJ et al. Passive acoustic monitoring provides a fresh perspective on fundamental ecological questions. Funct. Ecol. 2023, Vol. 37, pp. 959-975. https://doi.org/10.1111/1365-2435.14275

7. Johnston P, Pierpoint C. Deployment of a passive acoustic monitoring (PAM) array from the AutoNaut wave-propelled unmanned surface vessel (USV). In OCEANS 2017-Aberdeen, 2017. IEEE. https://doi.org: 10.1109/OCEANSE.2017.8084780

8. Treloar AA et al. Real-time in-situ passive acoustic array beamforming from the AutoNaut wave-propelled uncrewed surface vessel. IEEE J. Ocean. Eng. 2024, Vol. 49, pp. 713–726. https://doi.org: 10.1109/JOE.2024.3365169

9. Da Silva Gomes S, Gomes SCP. A new dynamic model of towing cables. Ocean Eng. 2021, Vol. 220, p. 107653. https://doi.org/10.1016/j.oceaneng.2020.107653

10. Zhao Y, Li G, Lian L. Numerical model of towed cable body system validation from sea trial experimental data. Ocean Eng. 2021, Vol. 226, p. 108859. https://doi.org/10.1016/j.oceaneng.2021.108859

11. Guo L et al. A numerical investigation on quasi-static configuration and nonlinear dynamic response characteristics

of marine towing cable. Ocean Eng. 2021, Vol. 240, p. 110007. https://doi.org/10.1016/j.oceaneng.2021.110007

12. Sun FJ, Zhu ZH, LaRosa M. Dynamic modeling of cable towed body using nodal position finite element method. Ocean Eng. 2011, Vol. 38, pp. 529-540. https://doi.org/10.1016/j.oceaneng.2010.11.016

13. Lalu PP, Narayanan KP. Numerical simulation of two-part underwater towing system [Dissertation]. 2013. Cochin University of Science and Technology. http://dyuthi.cusat.ac.in/purl/3751

14. Minowa A, Toda M. Stability analyses on a towed underwater vehicle motion control system using a high-gain observer. Adv. Control Appl. Eng. Ind. Syst. 2021, Vol. 3, p. e77. https://doi.org/10.1002/adc2.77

15. Yang S, Zhu X, Ren H. Dynamic analysis of a deep-towed seismic system based on a flexible multi-body dynamics frame. Ocean Eng. 2023, Vol. 279, p. 114587. https://doi.org/10.1016/j.oceaneng.2023.114587

16. Guo L et al. Experimental investigation on vortex-induced vibration of marine towing cable with suppression device. Ocean Eng. 2023, Vol. 269, p. 113531. https://doi.org/10.1016/j.oceaneng.2022.113531

17. Guo L et al. Numerical investigation and arrangement optimization on VIV response of marine towing cable with suppression device. Mar. Struct. 2024, Vol. 95, p. 103598. https://doi.org/10.1016/j.marstruc.2024.103598

18. Guo L et al. Experimental investigation on nonlinear dynamic response of towing cable under vessel motion. Ocean Eng. 2022, Vol. 266, p. 113170. https://doi.org/10.1016/j.oceaneng.2022.113170

19. Zheng H, Wang J. A numerical study on the vortex-induced vibration of flexible cylinders covered with differently placed buoyancy modules. J. Fluids Struct. 2021, Vol. 100, p. 103174. https://doi.org/10.1016/j.jfluidstructs.2020.103174

20. Wang G, Rong B, Tao L, Rui X. Riccati discrete time transfer matrix method for dynamic modeling and simulation of an underwater towed system. ASME J. Appl. Mech. 2012, Vol. 79, p. 041014. https://doi.org/10.1115/1.4006237

21. Fritzson P, Pop A, Aronsson P et al. OpenModelica users guide. Simulation 2006, Vol. 82, pp. 109-150. http://www.ida.liu.se/projects/OpenModelica

22. Younesian D, Esmailzadeh E, Sedaghati R. Passive vibration control of beams subjected to random excitations with peaked PSD. J. Vib. Control. 2006, Vol. 12, pp. 941-953. https://doi.org/10.1177/1077546306068060